A temperature window of reduced flow resistance in polyethylene with implications for melt flow rheology: 1. The basic effect and principal parameters*

J. W. H. Kolnaar† and A. Keller‡
H. H. Wills Physics Laboratory, Tyndall Avenue, Bristol BS8 1TL, UK

This is the first of three papers on a recently discovered melt flow singularity during capillary flow of linear polyethylene, the 'extrusion window' at and close to 150°C. After placing the subject in its historical perspective, the various experiments are described by which the 'extrusion window' is revealed. These are: a minimum in pressure at around 150°C for constant material throughput and a maximum in material throughput at 150°C when a constant pressure level is maintained. In the former case the effect sets in at a critical piston velocity v_c (i.e. shear rate $\dot{\gamma}_c$) and in the latter case at a critical pressure p_c. The v_c value was found to be in a steeply inverse relation to molecular weight (M), obeying a power dependence of precisely -4, while p_c was practically independent of M. The singularity in melt flow behaviour in question is inexplicable in terms of continuum rheology and points to a thermodynamic origin, more specifically to a phase transition at the particular temperature. In line with previous work, the formation of a transient, hexagonal 'mobile' crystal phase is suggested, here created through flow-induced chain extension. While seemingly the criticality in v_c and the low end cut-off in M suggest the agency of elongational flow-induced chain stretching, such as is known to take place at the orifice entrance (a view held in the preceding publications), the newly found invariance of p_c with M now speaks decisively against the orifice being the site of initiation of the window effect. Rather, it points to a yield phenomenon, such as wall slip in the capillary, which itself would be the consequence of a chain-extension-induced phase transformation at the sharply defined temperature of 150°C, the plausibility of which is argued in this paper. Irrespective of the ultimate source of the effect, its potential advantage for certain melt processing operations should be apparent through requiring less energy for a given material throughput and by ensuring distortion-free extrudates under conditions where otherwise such distortions would be present. Other, more specific issues raised by the work include the relation of the newly found power law to the established M dependence of melt viscosity.

(Keywords: capillary extrusion; melt flow rheology; enhanced extrudability)

INTRODUCTION

Scope

In this series of three papers we report on an unusual melt flow effect observed during capillary extrusion of linear polyethylene (PE). The effect is a specific singularity in extrusion behaviour, occurring within a narrow temperature range of 1–3°C at around 150°C, which does not follow in any predictable way from conventional rheology. It is a major puzzle scientifically and, as it involves reduced flow resistance coupled with the absence of extrudate distortions, offers practical advantages in processing. The effect itself has been reported in several previous publications[1–4]. The present investigations, after consolidating the first reports, have taken the subject considerably further, opening new avenues for interpretation. The present series of papers will provide a comprehensive updating of this subject.

In this first part, the broader subject matter is placed in its historic perspective, followed by a description of the basic phenomena by which the new effect has been recognized and the relevant variables affecting it, including details and qualifications not reported so far. Completely new experiments are then described, leading to the recognition of new relationships which necessitate a revision of our own viewpoint adopted so far. All of the experiments in part 1 consist of measuring flow properties as a function of temperature within a fixed capillary die geometry.

In the experiments of part 2, the geometry of the flow will be altered in a systematic manner and, in addition, rheological investigations will be described at constant temperature. Part 3 will be concerned with the nature and origin of flow instabilities arising from the sum total of this series of investigations.

Historical

The specific effects in question are part of a broader subject area, namely melt flow slightly above the

*Presented at 'Polymer Science and Technology—a conference to mark the 65th birthday of Professor Ian Ward FRS', 21–23 April 1993, University of Leeds, UK

† Permanent address: DSM Research BV, PO Box 18, 6160 MD Geleen, The Netherlands

‡ To whom correspondence should be addressed

0032-3861/94/18/3863–12

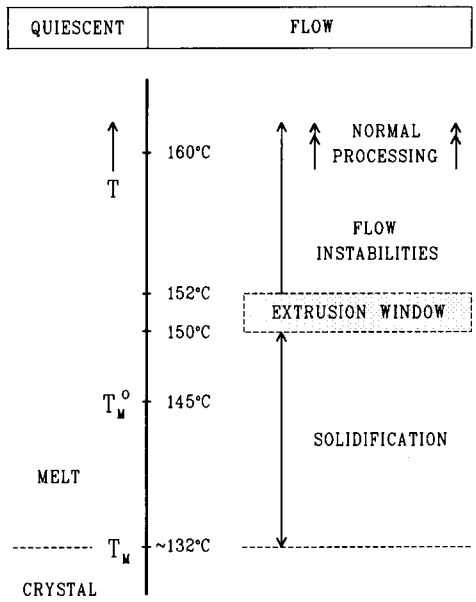

Figure 1 Temperature scale for melt flow of linear polyethylene in a capillary extruder. The scale on the left pertains to the quiescent state (T_m = practical melting temperature; T_m^0 = theoretical melting point of an infinite crystal). The scale on the right applies to melt flow such as leads to solidification and displays the 'extrusion window'

solidification point of the polymer, in this case PE. In the case of linear PE, solidification (crystallization) normally sets in between 120 and 130°C on cooling, depending on the cooling rate, while on heating a solidified product, melting sets in at 132–136°C (practical melting point) with the maximum (theoretical) melting point generally held[5,6] to be at 145°C. Conventional melt processing is usually conducted at much higher temperatures, i.e. at 160°C and above, to avoid any possible interference of the solid state with melt flow (see annotated temperature scale of *Figure 1*). In contrast, the subject matter of present concern is melt flow within the range where such an interaction can occur, not only because of its intrinsic scientific interest, but also because processing at these lower temperatures can be advantageous, either by virtue of melt properties[1-4] or properties of the resulting solidified product[7-11].

In the following, a simplified history of the subject area, namely melt extrusion and its consequences at such 'low' temperatures, is outlined. The experiments quoted all involve a capillary rheometer consisting of a converging die entry (see *Figure 2*) and a capillary following it, used either as a viscometer to measure melt flow properties or as an extruder for obtaining an extrudate.

To our knowledge, the first publication of relevance is that by van der Vegt and Smit[12], who measured melt viscosities (η) of polypropylenes (PP), PE and other polymers, in an apparatus such as that shown in *Figure 2*, at chosen constant temperature (T) as a function of shear rate ($\dot{\gamma}$), which for a fixed capillary geometry means piston velocity (v). While equally valid for PP (and other crystallizable polymers), the following discussion is limited to PE, for the sake of relevance to our own work. At temperatures above ~155°C the melt viscosities followed the normal pattern (i.e. decreasing η with increasing T and, for a given T, decreasing η with $\dot{\gamma}$, i.e. shear thinning behaviour). At lower temperatures anomalies were observed. Thus at and beyond a critical $\dot{\gamma}$ ($\dot{\gamma}_c$ = critical shear rate), η increased sharply and could eventually rise to infinity, which means that the flow within the capillary became blocked. *Figure 3* illustrates our own version of the effect described in ref. 12, where it is expressed in terms of viscosity (η) vs. shear stress (τ), which is less suited for our purpose here. While 146°C is far below the usual processing temperature range, it is still considerably above the temperature at which a PE melt is expected to crystallize (see *Figure 1*) (an analogous effect is found with PP and other polymers at corresponding temperatures).

Van der Vegt and Smit interpreted the departure from the expected shear thinning behaviour as due to orientation-induced crystallization, which could take place at temperatures higher than the normal crystallization

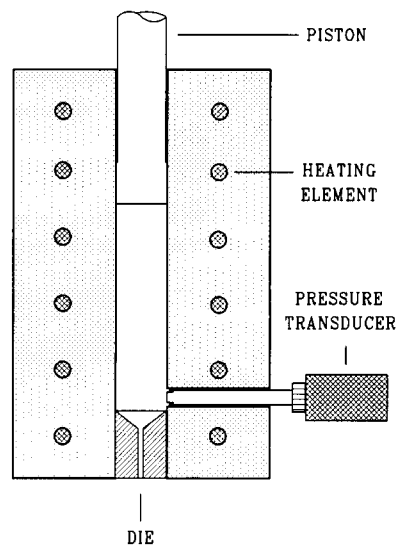

Figure 2 Schematic representation of the capillary rheometer used in extrusion experiments

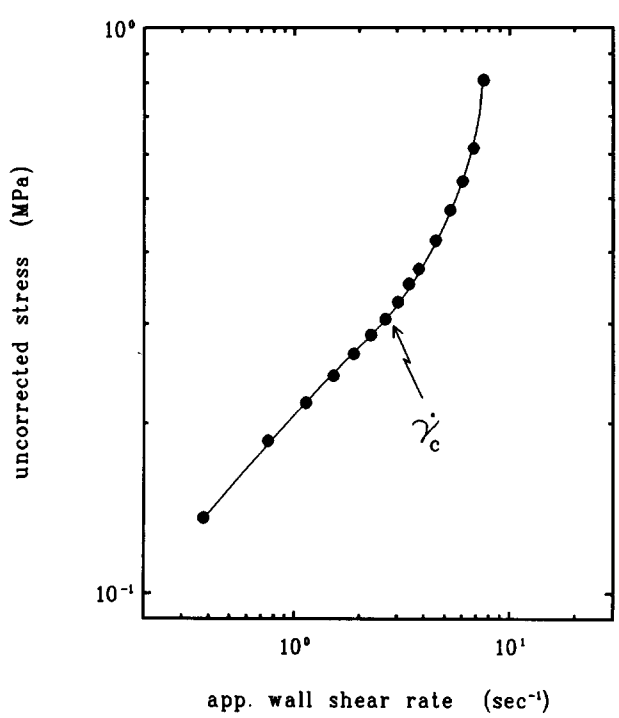

Figure 3 Apparent flow curve (uncorrected stress vs. apparent wall shear rate) for a linear polyethylene ($M = 2.8 \times 10^5$) measured at 146°C, showing the onset of elongational-flow-induced crystallization (indicated by $\dot{\gamma}_c$)

temperature in the isotropic melt, and in fact could exceed the theoretical melting point in the quiescent state (i.e. 145°C). Indeed, the solidified plug extracted from the capillary was found to be unusually highly oriented. The orientation itself was attributed (correctly, as we now know) to the chain stretching effect of the elongational flow arising through converging flow at the die entrance. The latter was supported by experiments performed with different die entry geometries: $\dot{\gamma}_c$ was higher for smaller die entry angles (α) and vice versa, in both qualitative and (to a first approximation) quantitative agreement with the expectation that smaller α means less convergence, hence a weaker elongational flow component for a given $\dot{\gamma}$ (hence throughput). In fact, for all but the highest α values ($2\alpha = 180°$, i.e. flat entry) the expectation was quantitatively fulfilled, i.e. $\dot{\varepsilon}_c \propto \dot{\gamma}_c \tan 2\alpha = \text{constant}$, proving that elongational flow, hence the die entry, is the source of the effects in question. This important experimental result and ensuing conclusion will be invoked again in connection with the new works later (part 2 of this series).

The central point of ref. 12 was essentially rheological. In subsequent works, taking up the above theme, the emphasis shifted to the structure and the properties of the extrudate. In the first instance this was the plug initially blocking the capillary, but in subsequent works this was squeezed out continuously in a kind of solid-state extrusion or in the form of a highly viscous partially solidified melt. As recognized in numerous works by Porter and co-workers (e.g. refs 13 and 14) such extrudates had advantageous properties: they were transparent and had exceptionally high modulus (for solidified plugs up to 200 GPa) with obvious consequences for application. The underlying structure was found to be fibrous, clearly a consequence of chain extension, locked in the form of fibrous crystals by crystallization, thus containing the chains in an essentially extended form.

Subsequent extensive work at the H. H. Wills Physics Laboratory[7-11] continued to focus on the resulting extrudate, 'fine tuning' the morphology by what may be termed 'micromorphological engineering'. This utilized the fact that the chain extension occurred only within a small portion of the material, namely in the high molecular weight (M) tail, the rest of the molecules, constituting the bulk of the material, remaining unextended to crystallize subsequently as lamellar overgrowth onto the fibrous crystals forming from the highest M material. This creates a two-component morphological system, where one of the components originates from the fully aligned and the other from the essentially still random chains, with no intermediate stages of alignment being involved (an issue to which we have recently given special emphasis[15]). The micromorphological engineering consisted of the purposeful variation of the ratio and interaction of the two components. Thus, under judiciously chosen circumstances, the lamellae growing out transversely from different fibres could interlock, giving rise to high modulus material (up to 100 GPa in static and up to 30 GPa in continuous extrusion experiments), but without some of the undesirable features of purely fibrous high modulus material, such as extensive fibrillation and heat shrinkage. Both the purely fibrous extrudate and extrudates with two-component fibre–platelet structures rely on elongational-flow-induced chain extension at the die entry for their existence. In recent years the concepts developed in H. H. Wills Physics Laboratory have also been adopted in injection moulding processes, aiming to improve the strength of the polymer. Moulding processes have been developed that introduce elongational flow along the injection direction to induce orientation and pressure in the flow channel for fixing the resulting shish-kebab morphology[16,17].

The new work in the present series reverted to re-examination of melt flow properties, that is rheology, at or just before the stage when the above-mentioned structures started forming. The new, unexpected phenomena arose in the course of these investigations.

EXPERIMENTAL

The majority of the experiments consisted of measuring pressure (p) as a function of temperature (T) at a constant piston velocity (v). For this purpose a Davenport capillary rheometer (Daventest Ltd) was used, connected to a home-constructed temperature programming system. Extrusion pressures were measured using a pressure transducer located a few millimetres upstream of the die, as shown schematically in *Figure 2*. A temperature measuring probe was fitted within the reservoir wall at the location of the die entrance. The barrel diameter was 10 mm and a cylindrical, stainless steel die was used, having an entrance with $2\alpha = 90°$ and a length/diameter ratio, $L/D = 14/2$ (mm/mm).

Two types of experiment were performed. In the first set of experiments, extrusion was started at a fixed extrusion rate at the preselected temperature. When the pressure had levelled off, either a heating or cooling run was performed at a rate of $\sim 1°C\,min^{-1}$ while maintaining a constant piston velocity; such experiments are referred to as 'dynamic'. In the second type of experiment, pressure traces were recorded as a function of time, at a fixed piston velocity, while keeping the barrel temperature constant; these are referred to as 'static' experiments*.

Samples were prepared for extrusion in the rheometer barrel by compaction of the powder at ambient temperature and melting at 180°C (30 min) to erase the nascent grain structure. After melting was completed, the barrel was cooled to preselected temperatures at which the polymer was conditioned for 15 min prior to starting the experiment.

Besides extrusion experiments at a fixed extrusion rate, experiments were also performed while maintaining a constant pressure drop over the extrusion die. For this purpose a Göttfert Rheograph 2002 capillary rheometer was used. The barrel diameter was 12 mm and the capillary die geometry was similar to that described above for the constant rate experiments. A constant pressure level was maintained using a proportional integral derivative (PID) controller. Extrusion was commenced at ~165°C and, after a constant extrusion rate was

* In the static experiments the measured temperature in the barrel will be close to the temperature at the wall, i.e. where the melt is in contact with the reservoir. (In fact it will be shown below that it is the effects near the wall, hence the temperature there, that is of consequence.) However, in the dynamic mode of experimentation there will be a radial temperature gradient across the rheometer barrel. When heating, this will lead to measured temperature values that are slightly higher than the temperatures at the wall. With regard to the accuracy of the temperature measurement, it is noted that closely similar temperature values (within 1°C) were found for the effects to be reported using a different apparatus. The dynamics of the heating and cooling runs will be commented on below

Table 1 High density polyethylene samples used in extrusion experiments

Polyethylene[a]	M_w (g mol^{-1})	M_w/M_n	Supplier
Rigidex 006-60	1.30×10^5	5.9	BP Chemicals Ltd
LAHD 01	4.40×10^5	4.9	BP Chemicals Ltd
HD6720 pr200	2.80×10^5	7.5	DSM
A	2.62×10^5	3.1	DSM
B	3.81×10^5	5.1	DSM
C	7.08×10^5	6.5	DSM
D	1.0×10^6	4.2	DSM

[a] Experimental grades A–D have approximately 0.15 CH_3 per 1000 C atoms

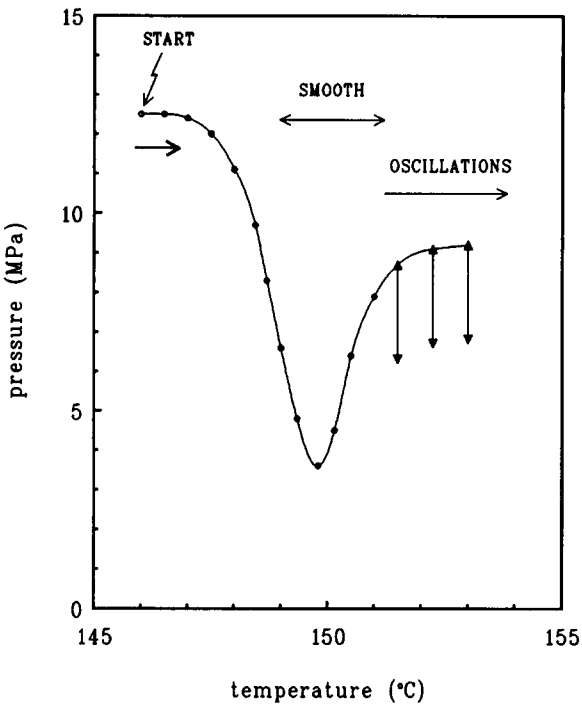

Figure 4 Pressure vs. temperature trace recorded during heating at a fixed extrusion rate showing the pressure minimum associated with the 'extrusion window'. The vertical arrows denote oscillations in pressure ($v = 1.25$ mm min^{-1} ($\dot{\gamma}_A = 1.89$ s^{-1}), heating rate 1°C min^{-1}, $M = 4.4 \times 10^5$)

attained, a cooling run was performed at a rate of ~ 1°C min^{-1}. While cooling, piston displacement rates were measured as a function of temperature and data were stored in a computer. The sample preparation procedure was analogous to that outlined above.

In the various capillary extrusion experiments, both commercial and experimental grades of PE were used. The weight average molecular weights (M_w) and polydispersity (M_w/M_n), as determined by gel permeation chromatography, are given in *Table 1*.

RESULTS

The basic effect

The basic effect, as described in previous publications[1–4] and here recalled from the present more consolidated viewpoint is as follows. The molten material is extruded with a constant piston velocity under a continuously varying temperature (T), with the pressure (p) being recorded. For appropriately high molecular weight (M) and for a sufficiently high piston velocity (v), both specified below, there is a sharp minimum in p within a narrow T range of 150–152°C. A p vs. T trace displaying this effect is depicted in *Figure 4* for the case of a heating run.

Even at this point the potential importance of the newly recognized effect is apparent, as the minimum in p means that less energy is required to process material in the narrow temperature range in question, referred to as the 'temperature window', compared with the conventional higher extrusion temperatures. But the advantages of working in the window go beyond the lower p value itself, both in terms of constancy of extrusion pressure and uniformity of the extrudate itself.

The high M materials, for which the effect is most pronounced, may usually display oscillations in p when extruded at these rates at conventional (high) processing temperatures. In the heating experiment the oscillations are absent up to the upper edge of the window (~ 152°C), at which stage they first appear. In the reverse experiment on cooling, they are present to begin with but disappear when the upper edge of the window is reached.

The singularity of the window is even more strikingly apparent from the appearance of the extrudate. For the high M values in question, and for practicable v values, the extrudates display non-uniformities and gross distortions of various kinds under the usual processing conditions. Several of these are absent within the T window where the extrudate is smooth. More will be said on such flow instabilities and extrudate distortions in part 3; at this stage *Figure 5* illustrates the effect, showing a photograph of an extrudate where the temperature was raised during extrusion. The smooth region corresponding to the extrusion temperature of ~ 150°C, in contrast to the gross distortions both below and above this temperature, should be strikingly apparent.

Above, we focused attention mostly on the T region above the window, as it is along this direction that we are approaching conventional processing conditions. When going in the direction of lower T we are approaching conditions of solidification. This is the region of previous work, leading to the various fibre–platelet morphologies[7–11] and eventual blockage of flow through massive solidification into a predominantly fibrous crystalline structure. When this occurs, the p trace is rising, as expected (p rises towards lower T in *Figures 4, 7* and *10* (see below), eventually swinging up towards

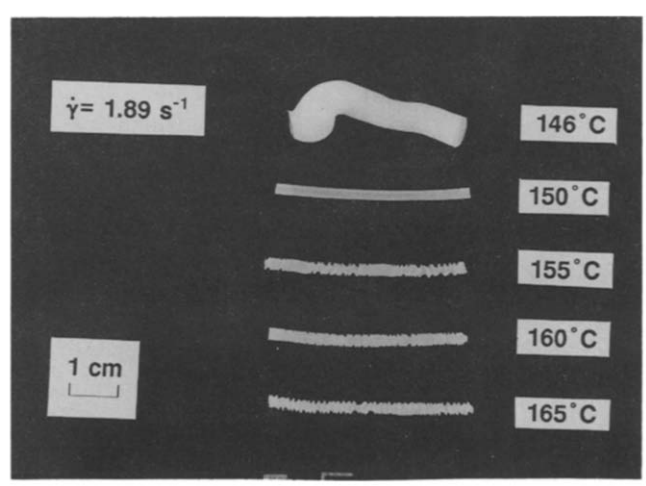

Figure 5 Photograph of extrudate obtained during a heating run corresponding to the pressure vs. temperature trace of *Figure 4*. Barrel wall temperatures are indicated

'infinity' when flow stops). In spite of this rise of p with decreasing T on crystallization, the p vs. T trace remains smooth compared to the oscillations at the high T side of the window. This would also apply to the appearance of the extrudate if it were hauled off at sufficient speed. If this is not done, as in our experiment, there is pronounced die swell on exit, particularly at T below the window; hence again the extrudate becomes grossly non-uniform, as conspicuously apparent from *Figure 5*. In the window itself die swell is minimal, again displaying the special advantage of the window condition. The die swell reappears at T above the window minimum, but being compounded there with the various other kinds of distortion, it is not as easy to recognize and even less easy to quantify. Even so, the transition from a smooth extrudate within the temperature window to a distorted one at higher T is gradual. When moving from the minimum in *Figure 4* towards higher T, a certain degree of quantification of die swell vs. T could be achieved up to a certain maximum T, which is $\sim 150°C$ in *Figure 6*. A minimum in die swell within the temperature window is clearly apparent (there is a slight difference in window temperature, i.e. 149 compared to 150°C in *Figure 4*; see below).

It will be apparent from the above that the existence of the window offers potentially significant advantages for processing that involves melt flow through orifices. The advantages are: less energy for a given throughput, uniform pressure and, chiefly, uniform extrudate under conditions where non-uniformity would otherwise prevail and in fact could make the manufacture of unidirectional products, such as monofilaments, rods and pipes, impractical if not impossible. In addition to the above practical considerations, understanding of the origin of the window effect poses a significant scientific challenge, to be addressed by much of the work to follow.

As implied by the above, the window effect arises both on heating (*Figure 4*) and on cooling. Nevertheless, this

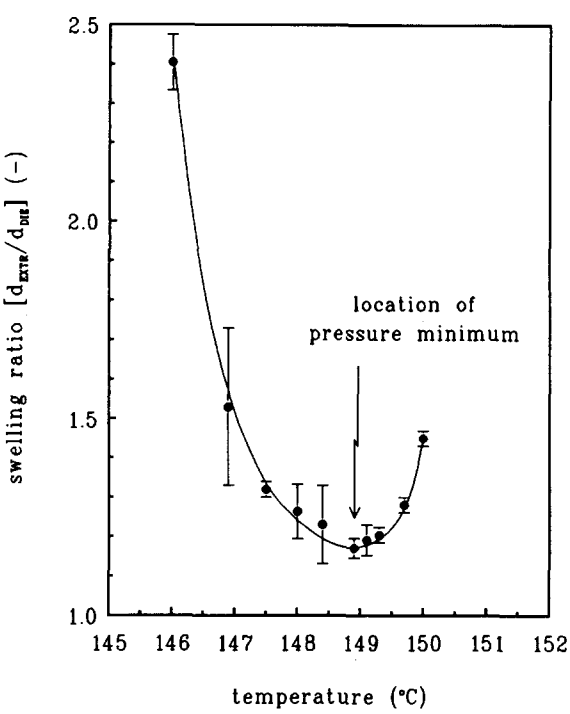

Figure 6 Swelling ratio as a function of temperature for isothermal extrusion experiments at a fixed piston velocity ($v = 1.25\,mm\,min^{-1}$ ($\dot{\gamma}_A = 1.89\,s^{-1}$), $M = 4.4 \times 10^5$)

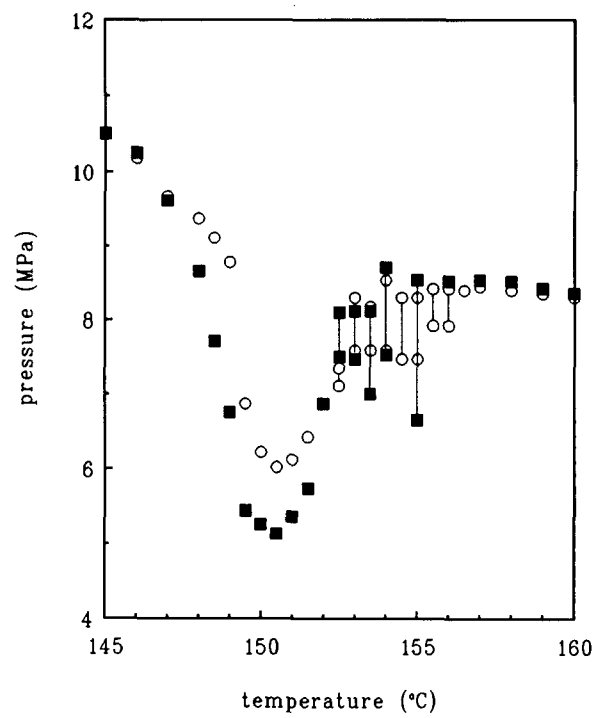

Figure 7 Pressure vs. temperature traces showing the pressure minimum for repetitive heating runs (○, first run; ■, second run). Vertical lines indicate pressure oscillations ($v = 2.5\,mm\,min^{-1}$ ($\dot{\gamma}_A = 3.78\,s^{-1}$), heating rate $1°C\,min^{-1}$, $M = 2.8 \times 10^5$)

reversibility is not quite unconditional, as already described in ref. 2. To recapitulate, the window effect (i.e. p minimum at 150–152°C) always appears on heating, but it does not always appear on cooling, and if it does appear it is not always in the same strength (i.e. same magnitude of the p drop). Specifically, if, after a given heating run, cooling starts immediately after the highest T ($\sim 180°C$) is reached, the window effect usually reappears with the same strength on cooling. In contrast, if the system is held at the highest T (say 180°C) for some time and the pressure is allowed to decay to zero, the window effect may be absent altogether. Similarly, if a cooling run is started from the high T end (say 180°C), without a preceding heating run, then depending on extrusion rate the window may or may not appear. As recognized in ref. 2 this 'conditional' reversibility has all the hallmarks of a memory effect, namely that a particular structure ('phase', see later) is created by the flow that is responsible for the window effect. This always happens on heating, but needs to be nucleated on cooling, a process much aided if some memory of the structure still exists. Accordingly storage at the elevated temperature, before cooling starts, could erase this memory effect, and of course in the absence of any previous heating run such memory would be non-existent altogether. In either case, renucleation of the structure in question would be required. This view has been confirmed by ongoing work, which has found that even when considering heating runs only the 'strength' of the effect (i.e. the depth of the p minimum) increases on repeated heating runs (see *Figure 7*). This effect of conditional reversibility with the underlying argument will be invoked again in parts 2 and 3.

On the exact temperature of the p *minimum*

We have noted that the window is very narrow, specified as 150–152°C, with the p minimum itself close

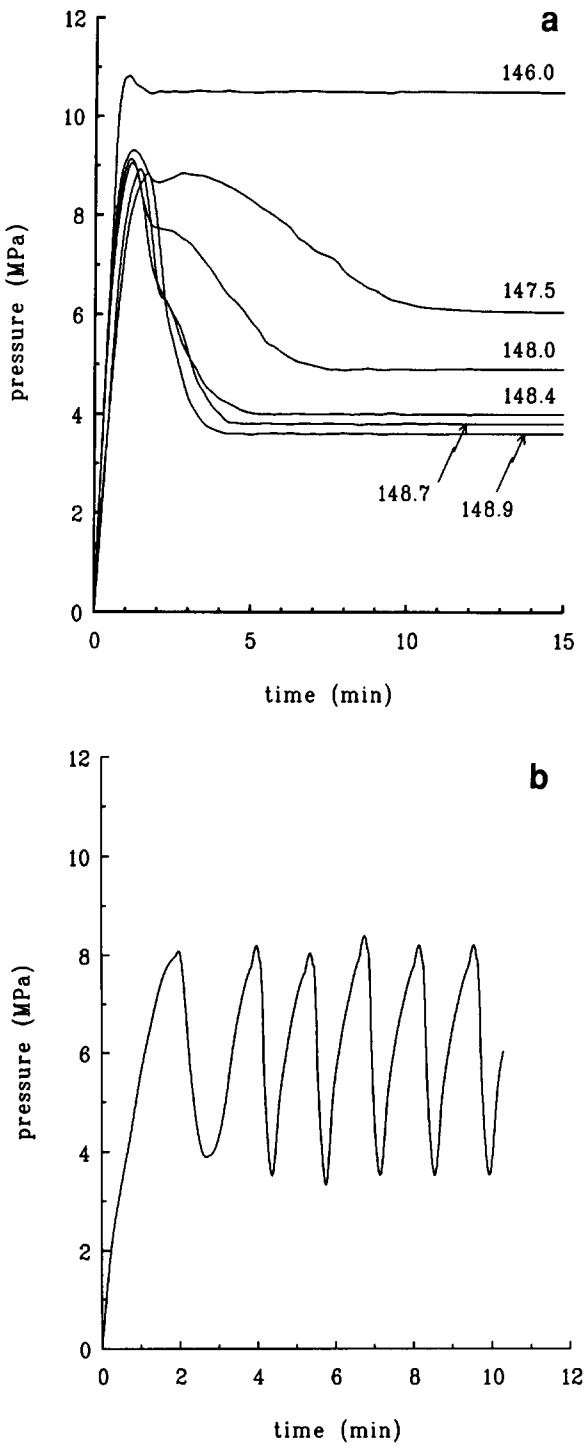

Figure 8 (a) Pressure vs. time traces recorded at different constant extrusion temperatures (in °C), showing decreasing pressure levels with increasing temperatures ($v = 1.25$ mm min^{-1} ($\dot{\gamma}_A = 1.89\,s^{-1}$), $M = 4.4 \times 10^5$). (b) Pressure vs. time trace as in (a) recorded at 150.5°C, showing oscillation in pressure as a function of time

to 151°C. In the kinds of experiment described, this numerical assignment seemed to be upheld with remarkable consistency. Even so, in *Figure 6* we have pointed to a slightly lower value of 149°C. The reason for such differences lies in the experimental procedure adopted, to which we shall now briefly turn.

All the previous experiments leading to the 151°C value were 'dynamic' experiments, where the p trace was taken in the course of continuously varying temperature, the rate of heating or cooling being ~ 1°C min^{-1}. Although this is a very slow rate, full thermal equilibration during the temperature changes cannot be guaranteed in view of the large thermal mass of the relevant parts of the extrusion apparatus. Clearly, variation of heating (or cooling) rates would be desirable, but with existing practicalities this could only be done within comparatively narrow limits (i.e. 0.5–5°C min^{-1}), for which no significant changes in window minimum temperature could be observed (i.e. the temperature corresponding to the pressure minimum shifted only by ~ 1°C, which is attributed to thermal inertia, as laid out in the footnote in the Experimental section; for the dynamic experiments, a rate of 1°C min^{-1} was chosen). For this reason, the 'static' experimental approach was adopted, the particulars of which are described in the Experimental section.

Figure 8a shows a characteristic example of extensive material in which the 'static' mode was employed. Here, after thermal equilibration at the chosen T, the piston was set in motion with a particular velocity (v) which, from preceding dynamic experiments (such as *Figure 4*), was known to give rise to the window effect, and p was monitored as a function of time (t). After a sharp initial rise (all within ~ 1.5 min for the extrusion rate employed) required for the flow to be started up, p immediately reached a constant value at the lowest T in *Figure 8a* (i.e. 146.0°C). In contrast, at higher T, approaching 148.0°C, p first drops with t until it reaches a lower plateau value, which lies below that of the initial pressure rise. The temperature associated with this plateau reaches a minimum value for runs close to 149°C. Further rise of T beyond 149°C leads to oscillations of p with t at the piston velocity of measurement, as depicted in *Figure 8b*.

The above type of experiment thus confirms the existence of the window effect (a p minimum in a narrow temperature range) by isothermal (i.e. static) experiments, thus complementing the dynamic experiments performed at continuously changing T. However, in such static experiment the T values for the window minimum are consistently lower, locating the minimum at ~ 149°C. Indeed, the minimum in die swell reported in *Figure 6*, the values of which are the outcome of such isothermal experiments, coincides with the p minimum of *Figure 8a*.

Regarding the absolute accuracy, the T values by the static experiments should lie closer to the true temperature for the p minimum. However, such experiments were more time-consuming to perform (many runs were needed to locate the window) and in any case, observations during heating and cooling are important in their own right. For this reason we shall adopt the dynamic mode of experimentation in much of the following, taking 150–152°C as the temperature of the p minimum, at the same time being aware that the 'true' value may be ~ 1°C lower. This reservation on the 'absolute' T value remains, regardless of the consistency of the experiments.

However, even within the confines of the dynamic modes of experiment, a small but systematic variation was observed with molecular weight (M). *Figure 9* shows that the higher M material gave slightly higher T_{min} values, a decade of M range leading to a rise in T_{min} of ~ 2°C. We attribute this effect to the change in melting point with M, which although small in this M range, nevertheless remains noticeable. It was established previously that T_{min} is significantly affected by introducing a small number of methyl branches (4.9 CH_3 per 1000 C atoms) into the PE chains[4] (for a PE with $M_v = 1.1 \times 10^6$,

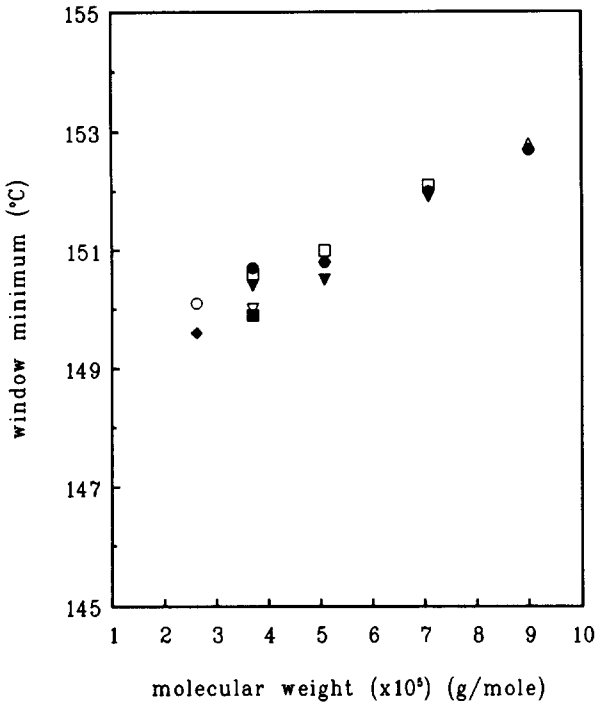

Figure 9 Location of the pressure minimum of the extrusion window as a function of weight average molecular weight (cooling run at $-1°C\,min^{-1}$). Piston velocities ($mm\,min^{-1}$): △, 1.00; ●, 1.25; □, 2.00; ▼, 2.50; ▽, 3.75; ■, 5.00; ○, 7.50; ◆, 10.0

T_{min} was found to drop by ~5°C). This effect was interpreted as being due to lowering of the crystal perfection by introducing short-chain branches, which in turn would raise the free energy of the crystal[18] and thus the phase transition temperature of the crystalline phase would be lowered. With the exception of the section explicitly dealing with the M dependence itself, most of the work described is on a single material with $M = 2.8 \times 10^5$ (this work and parts 2 and 3 of this series); hence the small effect of M dependence will not concern us further.

Finally, it can be observed from *Figure 9* that for a given M the location of the pressure minimum shifts to slightly lower T when the rate of extrusion is increased. For a low M in *Figure 9* (e.g. $M = 3.8 \times 10^5$), the drop in T_{min} is ~1°C when increasing the piston velocity from 1.25 to $5.0\,mm\,min^{-1}$ (i.e. a four-fold increase). At still higher rates, T_{min} appears to remain essentially unaltered (not shown in *Figure 9*). For the highest M values in *Figure 9* (i.e. $M = 7.1 \times 10^5$ and 9.5×10^5), the location of T_{min} does not vary at all with extrusion rate.

The effect of piston velocity (shear rate)

It has already been reported[2,4] that, for a given capillary die geometry, the window effect sets in only beyond a given piston velocity (v) or, equivalently, beyond a corresponding shear rate ($\dot{\gamma}$). This is now demonstrated from the current work (*Figure 10*), in the first instance for self-contained presentation to provide comparison with what is to follow, and secondly for the additional information it contains.

For the lower v values in *Figure 10*, p decreases steadily with T, a behaviour to be expected from decreasing viscosity of polymer melt with increasing T. However, at a sharply defined value of v (between 1.75 and $2.0\,mm\,min^{-1}$, i.e. within a range of only 14%), the sharp minimum in p close to 150°C appears, i.e. the effect identified with the extrusion window. On increasing v further (in the case illustrated, by ~20%), the minimum deepens dramatically, with its position along the T axis remaining essentially unaltered (it is questionable whether the slight shift of T_{min}, within 1°C, is significant or not). Previously we interpreted this indicating that the window effect (and the underlying molecular process) is critical in shear rate[2,4].

Here it will only be mentioned that there is an upper limit to the range of v where the extrudate is smooth and uniform, as beyond a certain v (hence $\dot{\gamma}$) a kind of flow instability (leading to the appearance of 'waviness' on the extrudate) sets in, even within the T window of the p minimum. This subject will be taken up specifically in part 3.

The window effect at constant pressure

In all the dynamic experiments displaying the window effect so far, the selected piston velocity was kept constant and variations in pressure were recorded as a function of temperature. In the following, the converse experiment is reported, where the pressure was maintained at a preselected level and the plunger velocity was measured as a function of temperature in a cooling run ($\sim 1°C\,min^{-1}$). The apparatus and relevant experimental conditions are described in the Experimental section.

Figure 11a displays what one may consider 'normal' behaviour, showing v as a function of T for three values of p. On lowering T, v falls, as expected from the increasing viscosity with decreasing T, corresponding to decreasing exit of fluid per unit time. The effect is larger for greater imposed constant p, which is to be expected. However, as p is increased beyond the value of 7.7 MPa, corresponding to the top curve in *Figure 11a*, a dramatic effect is observed, as shown in *Figure 11b*. Here, on a greatly condensed scale, the three lower curves correspond to

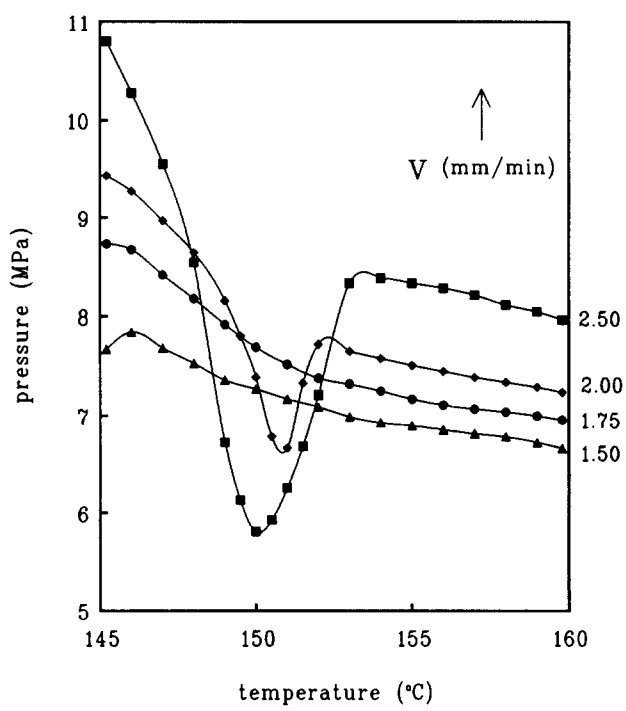

Figure 10 Pressure vs. temperature traces recorded during heating (at $\sim 1°C\,min^{-1}$) showing the influence of extrusion rate ($M = 2.8 \times 10^5$); piston velocities are indicated

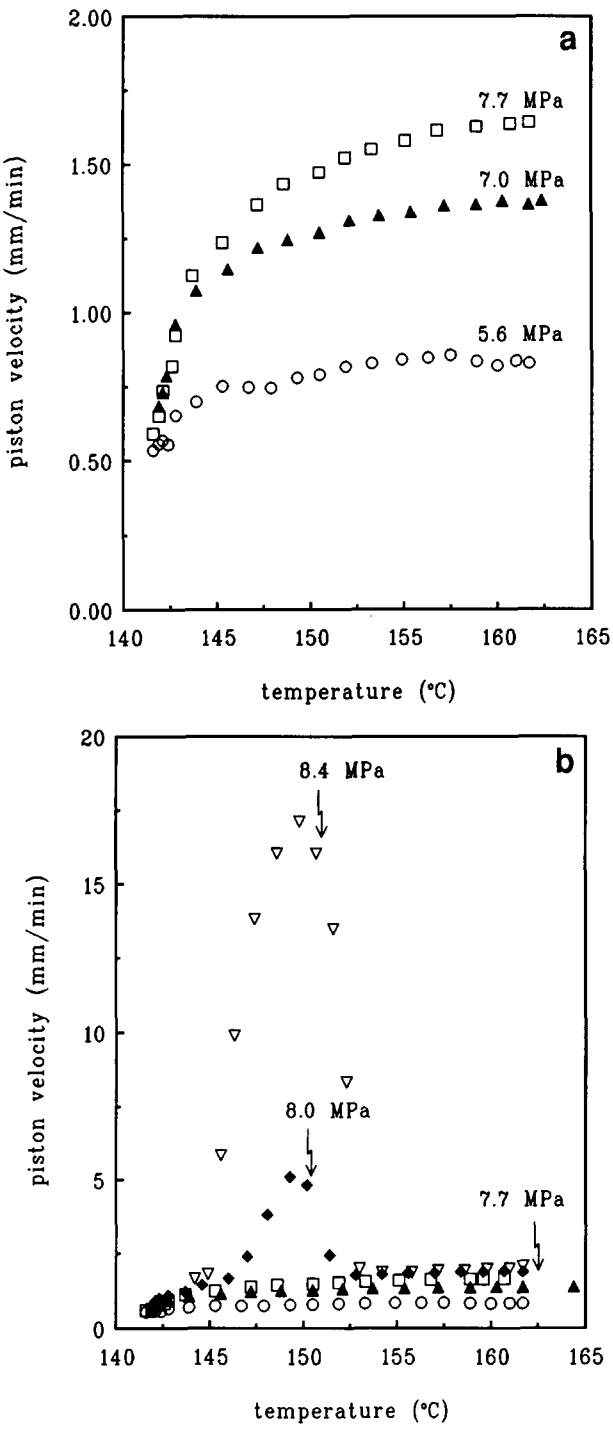

Figure 11 (a) Piston velocity vs. temperature plots recorded during extrusion at constant pressure. Pressure values increase from bottom to top (cooling run at $\sim 1°C\,min^{-1}$, $M = 2.8 \times 10^5$). (b) As in (a), but showing a sharp maximum in extrusion rate at $\sim 150°C$

those in *Figure 11a* displaying conventional behaviour. However, on a minute increase in p from 7.7 to 8.0 MPa, a sharp maximum in v appears at 150°C. On a further small increase of p to 8.4 MPa (i.e. by only about 5%) this maximum in v increases by a factor of about 3.5 with the correspondingly enhanced exit rate of fluid. On a further increase in p, v increased to such high values that a constant p could no longer be maintained by the apparatus.

These experiments, as displayed by *Figure 11b*, thus confirm the existence of a melt flow discontinuity in a temperature range at or close to 150°C. They demonstrate the same window effect, in this case in terms of a sharp maximum of plunger velocity at a constant p, as opposed to a minimum in p at a constant v. Just as v had to exceed a certain critical value for the minimum in p to appear (*Figure 10*), beyond which the minimum became rapidly more pronounced, here p had to pass a particular sharply defined threshold for the maximum in v to become apparent, increasing dramatically beyond this threshold value. The effects displayed by *Figures 10* and *11* are thus complementary, creating an all-round self-consistency in this family of experiments.

Effect of molecular weight

It was shown previously that the appearance of the window effect was strongly dependent on molecular weight; for a given v, M ($M \equiv M_w$) had to exceed a certain critical value for the effect to set in. Thus for conditions applicable in ref. 1, a given polymer of $M = 2.2 \times 10^5$ showed only normal extrusion behaviour (steady decrease in p with increasing T in line with decreasing viscosity), while for the same v a polymer of $M = 4.1 \times 10^5$ displayed the window effect in a highly pronounced manner, as did another grade of polymer with still higher M ($M = 9.5 \times 10^5$). Bearing in mind the broad M distributions of all these samples and the different distributions for the different grades, the above finding seemed to indicate to us that for a given v (i.e. $\dot{\gamma}$), the boundary in M for the effect to occur is sharply defined, hence the effect is 'critical' in M in addition to v (i.e. $\dot{\gamma}$). With the scarcity of available grades in the M range in question, we could not define the sharpness of the boundary in M more closely than the interval between the two grades quoted above.

We could define the M dependence more closely through the acquisition of grades within the range of $M = 1.3 \times 10^5$ to 1.0×10^6. While the polydispersity was unavoidably quite wide, $M_w/M_n \approx 5$–6 (see *Table 1*), it was generally the same for all samples over the full M range.

The experiments consisted of determining the threshold v value where the window effect set in for each M at a given capillary geometry ($L/D = 14/2$), as shown in *Figure 10*. Denoting v thus defined as v_c the results are represented by *Figure 12* in the form of a double logarithmic v_c vs. M plot. It is seen that (i) all points fall close to a straight line, and (ii) this straight line has a slope of -4.0 ± 0.1, identifying a power law relationship:

$$v_c \propto M^{-4.0 \pm 0.1} \quad (1)$$

At this stage we may remark that, bearing in mind the intrinsic complexity of the effect in question and the polydispersity of the materials used, the emergence of such a clear-cut effect is remarkable and indicative of some basic underlying cause.

As a next step we may consider the pressure value (p_c) for each v_c in *Figure 12*. A plot of p_c vs. M shows that the p_c values are all very close, at about 7.0 MPa (*Figure 13*). The points broadly define a horizontal line; even if there is some scatter about this line, the deviations are negligible compared to the huge variations in v_c over the same M range. We can assert, therefore, that while v_c varies steeply (power of -4) with M, p_c is, to a good approximation, constant over the same M range. As will be discussed below and taken up further in parts 2 and 3, the above findings signal the need for a new departure.

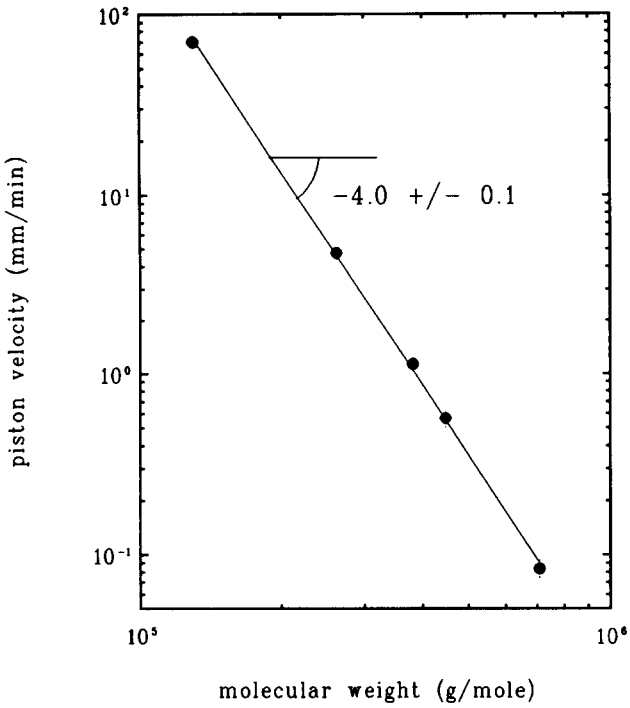

Figure 12 Critical onset piston velocity at the inception of the 'extrusion window' vs. weight average molecular weight as obtained from heating runs (heating rate 1°C min^{-1})

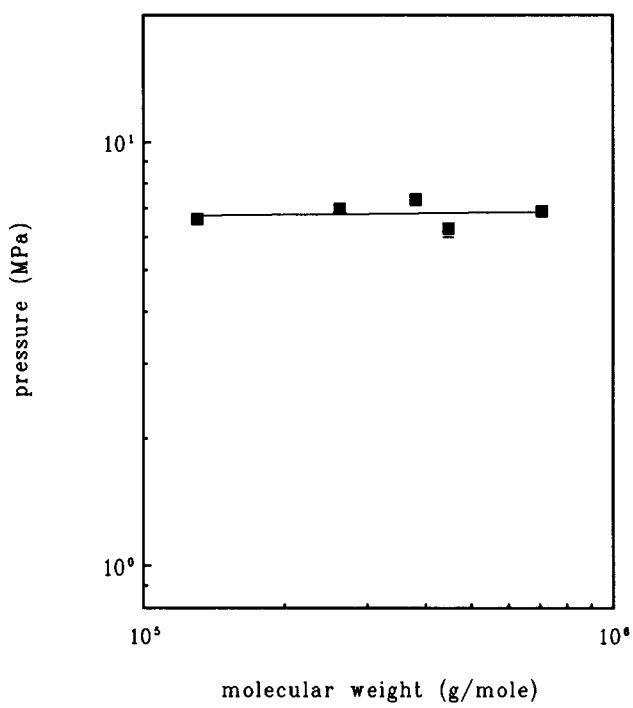

Figure 13 Critical pressure vs. weight average molecular weight as obtained from heating runs (heating rate 1°C min^{-1})

Some comments will now be made on the extremes of the range of molecular weights displaying the extrusion window effects, as depicted in *Figures 4–13*. For samples having M values much greater than those shown in *Figures 12* and *13* ($M > 9.0 \times 10^5$, i.e. ultrahigh molecular weight PE (UHMWPE) material) the pressure minimum was found to be absent when the sample preparation procedure detailed in the Experimental section was followed (even after prolonged heating at 180°C for up to 2 h). However, when a dried gel of the nascent UHMWPE powder* is processed in either a heating or a cooling run, a pronounced pressure minimum and a smooth extrudate were obtained. It was noted previously that a dried gel of UHMWPE ($M \approx 9.0 \times 10^5$) substantially promoted the occurrence of the pressure minimum compared with the nascent powder[3]. As has been recognized previously, this behaviour of very high M material can be attributed to the presence of a grain structure in the melt, even at the high temperatures employed (i.e. ~180°C), which are the residues of the original nascent morphology[11]. During dissolution of the nascent powder these grains are removed and do not reappear on gelation. We have thus shown that a nascent UHMWPE powder, which would otherwise not show the pressure minimum (or a sharp maximum in extrusion rate, depending on the mode of operation of the rheometer), does show the extrusion window when the nascent grain structure is removed by dissolution, gelation on cooling and drying.

At the low M side of *Figures 12* and *13* our lowest limit was $M = 1.3 \times 10^5$. At still lower M values, the extrusion becomes unstable for the correspondingly high v values required, and a constant plateau in the p vs. t curves, such as in *Figure 8a* for $T = 148.9$°C (i.e. for $M = 4.4 \times 10^5$), is no longer attained. We return to this point in part 3.

DISCUSSION

It was recognized early on that the window effect cannot be explained by continuum rheology of polymer melts alone, and more positively, that the sharp singularity with temperature points to a thermodynamic factor, a phase transition in particular. The results in the present paper lend further support to this contention: these are the uniqueness and sharpness of the effect, its clearly defined temperature range and the further evidence that memory effects may be operating. Previously the latter was indicated by the observation of conditional reversibility with heating and cooling, presently reinforced by the enhancement of the effect by repetition of the same heating runs.

The next question is the nature of the phase involved in the proposed phase transition. In analogy to the antecedents surveyed in the Historical section, a liquid to crystal transformation suggests itself. However, such a liquid to crystal transformation would increase the flow resistance, as opposed to decreasing it, which is the present effect. In fact the upswing of p towards low T at the low T end of the p minimum (see, for example, *Figures 4* and *10*) and the downturn of v at the low T end of the rate maximum in *Figure 11b*, is in fact due to crystallization, which indeed can lead to complete cessation of the flow, the effect first observed by van der Vegt and Smit[12]. Based on such considerations, the hexagonal phase of PE has previously been suggested as responsible for the window effect[1,2,4]. This hexagonal phase is known to contain chains in a highly mobile form and has liquid crystalline characteristics. This, in principle at least, could

* The dried gel was obtained by dissolution of the UHMWPE powder (sample D, $M = 1.0 \times 10^6$) in xylene at $T = 130$°C (at a 6 wt% concentration to which 1 wt% (based on polymer weight) antioxidant (Irganox) was added), followed by gelation on cooling and extraction of the solvent by drying at 60°C in a vacuum oven

account for the low flow resistance and for the absence of features, such as die swell, associated with elasticity of melts constituted by randomly interpenetrating molecules. This hexagonal phase is metastable at atmospheric pressure, but there is evidence that it can be produced as an apparently stable phase by, for example, holding the chains stretched by appropriately constraining ultradrawn fibres or flow oriented (shish-kebab) crystals[19–21]. In such cases the melting points (T_m) of all modifications are raised, but that of the metastable modification $(T_m)_h$ to a greater extent than that of the stable one $(T_m)_o$, with the result that a temperature range is created where the previously metastable phase becomes stable (subscripts o and h refer to orthorhombic and hexagonal phases in PE, respectively). In most previous experiments a temperature of about 150°C is recorded for an orthorhombic–hexagonal transition in such a constrained system, in remarkable coincidence with the present observation of the p minimum*.

This implies that the suggested phase transition is induced by the chains becoming stretched out in the course of flow, changing the free energy of the system in such a way as to 'uncover' the originally metastable hexagonal phase[18]. In other words, a situation is created that is analogous to that of the constrained fibre referred to above[19–21]. Having reached this stage of the argument, the preceding work envisages chain extension as arising through the effect of elongational flow, such as necessarily present at the orifice entry, already invoked to account for the crystallization–solidification effects (at the slightly lower temperature but still above the practical solidification temperatures) by van der Vegt and Smit, Porter, and by previous work in our laboratory. The present effect, although operating in the opposite direction (reduced instead of increased flow resistance), would fall naturally into this scheme by invoking the mobile hexagonal instead of the conventional orthorhombic phase as created at the particular temperature. Chain extension by elongational flow is known to be a discontinuous process, corresponding to a 'coil–stretch' transition, with no steady intermediate stage in between, itself critical both in strain rate and molecular weight, both pertaining to the creation of the present window effect (see, for example, ref. 15).

So far the argument seems self-consistent, its different aspects mutually supporting each other. However, one item, the constancy of p_c as a function of M (*Figure 13*) does not fall in line. Namely, it makes the window effect analogous to a 'yield' phenomenon, a run-away effect at a particular stress (τ_c) rather than the direct consequence of a critical strain rate (hence shear rate), as hitherto envisaged. Therefore, the suggested yield could be slippage of the material at, or close to, the solid boundary, converting a Poiseuille-type flow behaviour into, at least partial, plug flow within the capillary. It is readily envisaged, even in qualitative terms, that such a plug flow component could have the characteristics required by the newly found window effect, namely low flow resistance and absence of flow irregularities both in terms of the p vs. T trace and extrudate appearance.

Plug flow (or wall slip) is of course a familiar phenomenon in rheology. However, our present proposal by no means represents a downgrading of the window effect to a known, somewhat trivial, precedent. Specifically, all the previous ingredients of the picture remain. First, the need for a phase transition still remains, because without it there is no reason why plug flow should set in at a specific, sharply defined temperature. Secondly, the requirement for the hexagonal phase also remains, or at least for a phase that is 'slippery', consistent with it being 'mobile': crystals proper would block, not promote, flow by all previous experiments. The transition to the new phase at the particular temperature must be chain-extension induced, otherwise there would be no reason for a phase other than the orthorhombic crystal. Such a new phase may still arise in the elongational flow field of the constriction, as previously envisaged, but, as stated above, will only have an effect when it appears at or near the capillary boundary wall, where the flow is of simple shear character.

The question therefore arises as to whether such chain extension could also be expected at the walls. It is apparent qualitatively that this could be so in the case of chains that are adsorbed to the walls of the flow channel. This issue has arisen previously in connection with the formation of shish-kebabs, and of extended-chain-type fibres from solution by Pennings' surface growth method[23]. In the present case, however, we are dealing with melts where entanglements between chains adhering to the wall and the molecules within the flowing interior also need to be considered. This issue has been addressed by Brochard-Wyart and de Gennes[24] who, amongst others, identified not only the condition of chain extension of adsorbed molecules (in their particular model, widely spaced along the wall so as to prevent overlap of different adsorbed chain molecules) in the process of disentanglement from the bulk interior, but also that the phenomenon was critical in shear stress at the wall (they invoke a 'marginal state' in which slip velocities increase rapidly). While it is by no means established how the Brochard-Wyart–de Gennes model applies to our case, it is clear that the application of some previous considerations on chain extension in the elongational flow field at the orifice entry to simple shear flow conditions at the walls, when coupled with adsorption effects, is not *a priori* unjustified. Clearly, in this respect we are at the beginning of new departures in the understanding of melt flow in general, in which the role of chains at the wall film–bulk melt interface plays a crucial part, a subject to which de Gennes and associates are currently giving much attention. The theoretical considerations just referred to apply to melt flow in general. To explain our own window effect, an appropriate phase transformation would still need to be superposed, as discussed in the preceding paragraph.

The shift of emphasis from die orifice to capillary walls as the site of the relevant effects in our case was not foreseen. The possibility of elongational flow inducing chain extension in the orifice remains unquestioned, as this has been the origin of all past studies on solidification effects and of purposeful creation of specific micromorphologies by extrusion not too far above the static melting point. The new question that arises is the connection, if any, between those past works on solidification effects, attributed to elongational flow at the die entry, and the present window effect, which seems to be associated with processes occurring along the capillary wall in simple shear flow. While we have no answer to

* By applying external constraints all along the chains in finely divided ultrathin fibres, this transformation temperature may be raised[22]. However, we argue[15] that in the present type of experiment, in which load is transmitted by viscous flow, this stage of loading is not reached

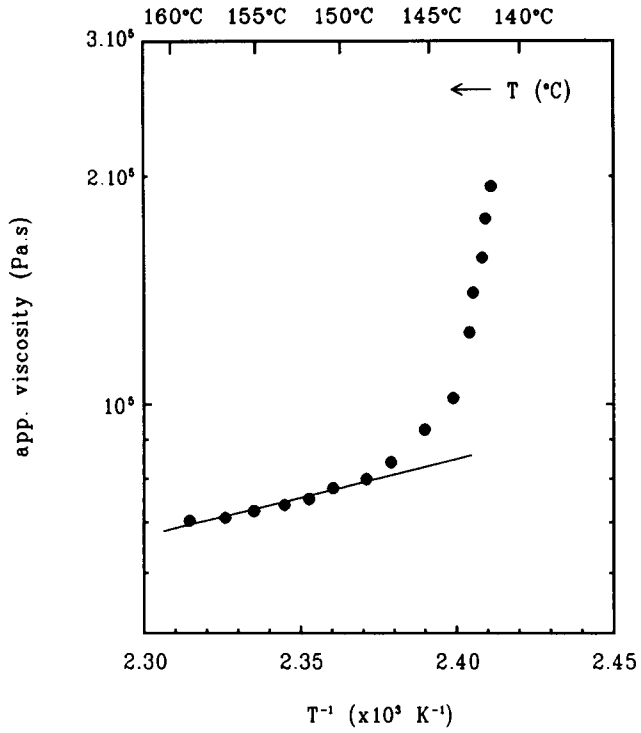

Figure 14 Logarithmic plot of apparent viscosity vs. T^{-1} showing elongational-flow-induced crystallization effects occurring at T below ~148°C

this particular question at present, we shall pursue the topic by separating the influences due to the die entry and to the capillary zone on the rheological behaviour in parts 2 and 3.

Finally, we end with some comments on viscosity arising from this work. By definition, shear viscosity is related to shear stress (τ) and shear rate ($\dot{\gamma}$) as:

$$\tau \equiv \eta\dot{\gamma} \tag{2}$$

For any discussion of viscosity we thus need to express results of measurement in terms of τ and $\dot{\gamma}$. In a capillary rheometer, τ and $\dot{\gamma}$ are related to the pressure drop ($\Delta p \equiv p - p^0 \approx p$) over the capillary die and to the material throughput (Q), respectively. For a given L/D ratio of the capillary, the shear stress (τ_w) exerted on the wall and apparent wall shear rate ($\dot{\gamma}_A$) are given by:

$$\tau_w = \frac{p}{4(L/D)} \tag{3}$$

and:

$$\dot{\gamma}_A = \frac{32Q}{\pi D^3} \tag{4}$$

respectively, in which Q can be calculated from the piston displacement rate (v) according to $Q = S_R v$, where S_R = area of cross-section of the reservoir.

It follows that in our case the measured quantities p and v relate to τ_w and $\dot{\gamma}_A$, featuring in the definition of η in equation (2), by respective multiplying factors which remain constant for the fixed geometry of our experiment. However, we need to qualify that by inserting p as measured into equation (3); we also include the pressure drop over the entrance and exit of the die. (The decomposition of total pressure drop into capillary drop and end losses will be the subject of parts 2 and 3.)

Equation (4) assumes Newtonian flow behaviour with a zero wall slip velocity at the wall. By referring to *apparent* shear rate ($\dot{\gamma}_A$) we treat the flow as if Newtonian. The magnitude of the departure from idealized Newtonian flow may be quantified by applying the Rabinowitsch correction[25]. The latter is only a slightly varying function of M, hence will not significantly influence the functional relations of our present concern, for which we shall retain $\dot{\gamma}_A$ in our discussion of η, referring to it as apparent viscosity (η_A).

In the light of the above, we may now express some of the p vs. T data in terms of apparent viscosities (η_A). Taking the top curve ($p = 7.7$ MPa) in *Figure 11a*, we obtain a η_A vs. T^{-1} plot expressed on a single logarithmic scale in *Figure 14*. We see that the curve is well approximated by a straight line at higher T (i.e. ~148°C < T < 160°C). This straight line is consistent with the familiar Arrhenius type of relationship between η and T, expressed by:

$$\eta = A\, e^{E_a/RT} \tag{5}$$

with E_a and R being the flow activation energy and universal gas constant, respectively. Taking the slope at high T we obtain $E_a = 19.3\ \text{kJ mol}^{-1}$, which is broadly consistent with expectations from melt flow in linear PE. The sudden upswing in η_A on lowering T at $T \approx 148$°C clearly does not follow from any continuum model of melt rheology, and implies a change in structure, in this case the onset of solidification. Indeed, it should be the same phenomenon as registered in *Figure 3*, originally observed by van der Vegt and Smit[12] and convincingly demonstrated as being due to crystallization, itself generated by elongation-flow-induced chain extension in the entry orifice. The present way of plotting in terms of η_A now identifies the onset of this crystallization with a temperature as high as 148°C for the conditions involved (M and constant τ). This upswing leads eventually to complete blockage of the flow when the temperature is lowered further.

Having established that, outside the conditions of solidification and up to the conditions of criticality for the 'window' effect, our data are interpretable in terms of conventional melt viscosity, we proceed to comment on the functional relationship of equation (1) in terms of viscosities. At the inception of the extrusion window, equation (2) corresponds to:

$$\tau_{w,c} = \eta_A \dot{\gamma}_{A,c} \tag{6}$$

From present experiments $\tau_{w,c}$ (i.e. p_c) does not depend on M; thus it follows from equation (6), by taking into account the inverse fourth power relation of v_c (hence $\dot{\gamma}_{A,c}$) in M (equation (1)), that:

$$\eta_A \propto M^{+4.0} \tag{7}$$

Now, for M sufficiently larger than the average molecular weight between entanglements ($M > M_e$), the empirically well established relation:

$$\eta_0 \propto M^{+3.4} \tag{8}$$

is known to hold (where η_0 refers to zero shear rate viscosity). The similarity between the power laws in equations (7) and (8) is clear. Nevertheless, equation (7) is held to be so well established and the accuracy of our fit is so high (see *Figure 12*) that the distinction between the exponents +3.4 and +4.0 needs to be accepted as real. The major difference between conditions leading to

equations (7) and (8) is that equation (8) refers to the limit of zero shear rate, while equation (7) embraces a huge range of shear rates, as represented by *Figure 12*. In view of the latter, the consistency of the straight line fit and the accuracy limits of the exponent +4.0 is rather remarkable and points to some profound underlying significance, an issue we are highlighting here without pursuing it further. In the latter connection we only remark that by conventional experience for finite shear rates, the exponent should fall below, and not exceed, +3.4, as we are finding currently, excluding the shear rate as an obvious connection between equations (7) and (8)[26].

CONCLUSIONS

The previously reported 'extrusion window' effect is now well established as a systematically recurring, highly reproducible feature in melt extrusion of linear PE. It should be advantageous for processing for two reasons: (i) less energy, stemming from a lower extrusion pressure, is required for a given material throughput, or conversely, higher material throughput for a given pressure drop, both effects here demonstrated by experiment; (ii) pressure oscillations and extrudate distortions are absent.

As an explanation, the previously suggested chain-extension-induced phase transition at the sharply defined window temperature, where the newly formed phase is 'mobile' (the hexagonal phase in PE) is being upheld. However, the observation of a molecular-weight-independent critical pressure is inconsistent with the source of the effect being in the orifice, and suggests the wall of the capillary as its likely location. The remarkable power dependence of precisely −4 of the critical piston velocity (i.e. shear rate) with molecular weight, points to some deeper underlying property of melts and calls for a correlation with power laws well established in the study of melt viscosities.

ACKNOWLEDGEMENT

Financial support of DSM, Geleen, The Netherlands, is gratefully acknowledged. The authors thank Professor P.-G. de Gennes for invaluable discussions and Mr E. Coenen for assisting in the extrusion experiments at constant pressure.

REFERENCES

1 Waddon, A. J. and Keller, A. *J. Polym. Sci.* 1990, **28**, 1063
2 Narh, K. A. and Keller, A. *Polymer* 1991, **32**, 2512
3 Narh, K. A. and Keller, A. *J. Mater. Sci. Lett.* 1991, **10**, 1301
4 Waddon, A. J. and Keller, A. *J. Polym. Sci.: Part B: Polym. Phys.* 1992, **30**, 923
5 Flory, P. J. and Vrij, A. *J. Am. Chem. Soc.* 1963, **85**, 3548
6 Wunderlich, B. and Czornyj, G. *Macromolecules* 1977, **10**, 906
7 Keller, A. and Odell, J. A. *J. Polym. Sci., Polym. Symp.* 1978, **63**, 155
8 Odell, J. A., Grubb, D. T. and Keller, A. *Polymer* 1978, **19**, 617
9 Bashir, Z., Odell, J. A. and Keller, A. *J. Mater. Sci.* 1984, **19**, 3713
10 Bashir, Z., Odell, J. A. and Keller, A. *J. Mater. Sci.* 1986, **21**, 3993
11 Bashir, Z. and Keller, A. *Colloid Polym. Sci.* 1989, **267**, 116
12 van der Vegt, A. K. and Smit, P. P. A. *Adv. Polym. Sci. Technol., Soc. Chem. Ind.* 1967, **26**, 313
13 Porter, R. S. and Johnson, J. F. *Trans. Soc. Rheol.* 1967, **11**, 259
14 Southern, J. H. and Porter, R. S. *J. Appl. Polym. Sci.* 1970, **14**, 2305
15 Keller, A. and Kolnaar, J. W. H. *Prog. Colloid Polym. Sci.* 1993, **92**, 81
16 Bayer, R. K., Baltá Calleja, F. J., López Cabarcos, E., Zachmann, H. G., Paulsen, A., Brüning, F. and Meins, W. *J. Mater. Sci.* 1989, **24**, 2643
17 Ehrenstein, G. W. and Maertin, C. *Kunststoffe* 1985, **75**, 105
18 Keller, A. and Ungar, G. *J. Appl. Polym. Sci.* 1991, **42**, 1683
19 Pennings, A. J. and Zwijnenburg, A. *J. Polym. Sci., Polym. Phys. Edn* 1979, **17**, 1011
20 Hikmet, R., Lemstra, P. J. and Keller, A. *Colloid Polym. Sci.* 1987, **265**, 185
21 Lemstra, P. J., van Aerle, N. A. J. M. and Bastiaansen, C. W. M. *Polym. J.* 1987, **19**, 85
22 Rastogi, S. and Odell, J. A. *Polym. Commun.* 1993, **34**, 1523
23 Zwijnenburg, A. and Pennings, A. J. *Colloid Polym. Sci.* 1976, **254**, 868
24 Brochard-Wyart, F. and de Gennes, P.-G. personal communication, 1992
25 Rabinowitsch, B. *Z. Phys. Chem. Abt A* 1929, **145**, 1
26 McLeish, T. C. B. personal communication, 1993